

Comparison between PAM and DMT in a 200-Gb/s IM-DD System Considering the Interaction between Bandwidth Limit and Peak Power Constraint at Transmitter

Di Che

Nokia Bell Labs, Murray Hill, NJ 07974, United States
di.che@nokia-bell-labs.com

Abstract: We revisit the PAM vs DMT debate in a 200G-class IM-DD system. Distinguished from previous works, we study the interaction between bandwidth limit and peak power constraint in an IM transmitter with peak distortion, and involve DSP techniques like faster than Nyquist and entropy loading for a more comprehensive achievable information rate comparison. © 2022 The Author(s)

1. Introduction

Since digital signal processing (DSP) was introduced to intensity-modulation direct-detection (IM-DD) systems more than a decade ago, there have been extensive comparisons among different modulation formats, especially for pulse-amplitude modulation (PAM) and discrete multitone (DMT) [1-7]. The recent advance of 200-Gb/s IM-DD optics changes some conditions of the comparison. One major difference is the system will be more component bandwidth limited (BWL) instead of fiber dispersion limited, because future IM-DD applications will mostly be limited to below 10 km with the coherent technique being penetrated to shorter and shorter reach. DMT is commonly regarded to be advantageous over PAM to combat the BWL, but the advantage is narrowed down by the recently revived faster-than-Nyquist (FTN) PAM [8,9]. The peak-power constraint (PPC) of an IM-DD system perplexes the comparison further. On one hand, PAM has higher signal power over DMT under the same PPC owing to its lower peak-to-average power ratio (PAPR), leading to higher optical modulation amplitude (OMA); on the other hand, by replacing the traditional bit loading (BL) with entropy loading (EL), DMT can achieve a probabilistic constellation shaping (PCS) gain [10] which vanishes in most PAM systems under the PPC [11]. The sophisticated interaction among these factors calls for a revisit of the comparison between PAM and DMT. In this paper, we perform an achievable information rate (AIR) comparison for them in a typical 200G-class IM-DD system with PPC and BWL.

2. Experimental Setup

The comparison is made in an IM-DD system as shown in Fig. 1. The SiGe digital-to-analog converters (DAC) has a maximum sampling rate of 128 GSa/s and more than 60-GHz analog bandwidth. Combining a 66-GHz amplifier, the electronic transmitter has sufficient bandwidth to generate PAM signals up to 128 GBd at 1 sample per symbol (sps) without severe peak distortion. The external modulated laser (EML) integrates an O-band DFB laser with an electro-absorption modulator (EAM) with a 3-dB bandwidth of 32 GHz and an extended response towards 50 GHz. The inset shows the power response of the EML which is the dominant bandwidth limit of the transmitter. Without considering the dispersion influence, we evaluate all signals in the back-to-back condition. The receiver consists of a 70-GHz PIN

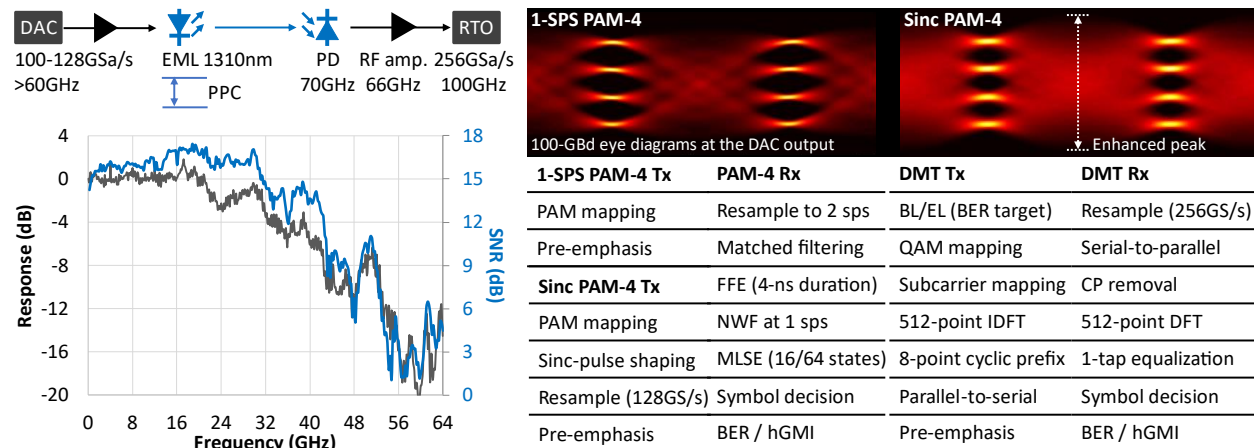


Fig. 1. Experimental setup and DSP flowchart. The left-bottom inset shows the power response (left axis) of EML and the end-to-end system SNR (right axis). RF amp.: (wideband) radio-frequency amplifier; Tx/Rx: transmitter/receiver DSP; hGMI: GMI under binary HD-FEC decoding [12].

photodiode (PD), a 66-GHz amplifier, and a 100-GHz real-time oscilloscope (RTO) at 256-GSa/s.

While the optics are likely part of the overall system BWL, it makes a big difference if the electronics (*e.g.*, DAC, driver) contribute to the BWL or not. When the electronics has little BWL like in our setup, PAM naturally has higher signal power (namely, OMA) than DMT under the PPC owing to its lower PAPR. In contrast, the stronger BWL the electronics suffer from, the higher PAPR a PAM signal exhibits. The additional DSP to combat the BWL like pulse shaping and pre-equalization may further enhance the PAPR. These peak distortion effects shrink the OMA advantage of PAM with respect to DMT. We emulate both types of PAM signal in this comparison. For the low-PAPR PAM, we generate variable symbol rate 1-sps signals from 100 to 128 Gbd by adjusting DAC sampling rates; for the high-PAPR PAM, we choose Sinc-pulse shaping as a peak distortion example and resample the signals (with symbol rates from 100 to 126 Gbd) to the fixed DAC speed at 128 GSa/s. An eye diagram comparison of the two at the DAC output is shown in Fig. 1. Note the 1-sps PAM also shows a little peak distortion due to the pre-emphasis. The 32-GHz 3-dB bandwidth of EAM makes all the PAM signals FTN. Thus, after the linear feed-forward equalizer (FFE), we perform FTN decoding combining a noise-whitening filter (NWF) and a maximum likelihood sequence estimator (MLSE).

Unlike PAM, DMT is not sensitive to peak distortion due to its high PAPR nature. We fix the DAC sampling rate at 128 GSa/s and the DFT size of 512 for DMT modulation, leading to the subcarrier spacing of 0.25 GHz. Each DMT symbol has 8-point cyclic prefix (CP). We include both BL and EL in the comparison. We choose a loading algorithm based on lookup tables [10] and select bit error rate (BER) as the loading target considering most IM-DD systems use hard-decision (HD) forward error correction (FEC) code. As the BWL has been accommodated by BL/EL, the receiver only has a linear frequency-domain equalizer with 1 tap per subcarrier.

We take some special cares on the DSP to provide an informative and fair comparison. First, we apply the same linear pre-emphasis filter to both PAM and DMT, whose coefficients are optimized for PAM considering DMT can use the adaptive loading to accommodate the colored system response. The end-to-end system SNR with pre-emphasis is shown in Fig. 1. Second, to provide an estimation of the lower-bound performance for PAM during its comparison with DMT, the distorted PAM signal (with Sinc-pulse shaping) is emulated to have the same electronic transmitter power penalty with the DMT signal by keeping an identical PAPR between the two. The PAPR control is realized by applying a higher digital clipping ratio (that induces neglectable demodulation penalty) to the DMT signal as its PAPR is higher than the Sinc PAM signal. Third, for a similar linear equalization performance at the receiver, we choose the FFE tap number as $512/128 \times SR$ where SR is the PAM symbol rate (GBd), corresponding to the time duration of a DMT symbol. This makes the FFE equivalent to the 1-tap frequency-domain equalizer with a DFT size of 512.

To avoid the influence from a specific FEC scheme, we select the generalized mutual information (GMI) under binary HD decoding as the AIR metric, calculated as $hGMI = \mathbb{H}(X) - \log_2 |\mathcal{X}| \cdot \mathbb{H}_2(\epsilon)$, where $\mathbb{H}(X)$ is the entropy of signal X and $\mathbb{H}_2(\cdot)$ is the binary entropy function, ϵ is the bit error probability and $|\mathcal{X}|$ is the size of the modulation alphabet [12]. The $hGMI$ of a DMT signal is the averaged value over all the subcarriers [10].

3. Comparison results

We illustrate the BER performance of various PAM signals in Fig. 2(a). Due to the BWL, signals after the linear FFE suffer from colored noise as shown in Fig. 2(c) for a 128-GBd signal. The NWF weakens such noise fluctuation from 12 to 6 dB, which greatly improves the symbol decision in Fig. 2(a) combining MLSE. Compared to the 1-sps PAM signal, the lower OMA of the Sinc-shaped signal degrades its signal-to-noise ratio (SNR) as shown in Fig. 2(b). This translates to larger BER for both cases with and without the FTN decoding.

To compare the AIR under different BER targets (in other words, HD-FEC thresholds), we evaluate the $hGMI$ of PAM and DMT signals as a function of measured BER, as shown in Fig. 3. We first compare the Sinc PAM-4 (w/o

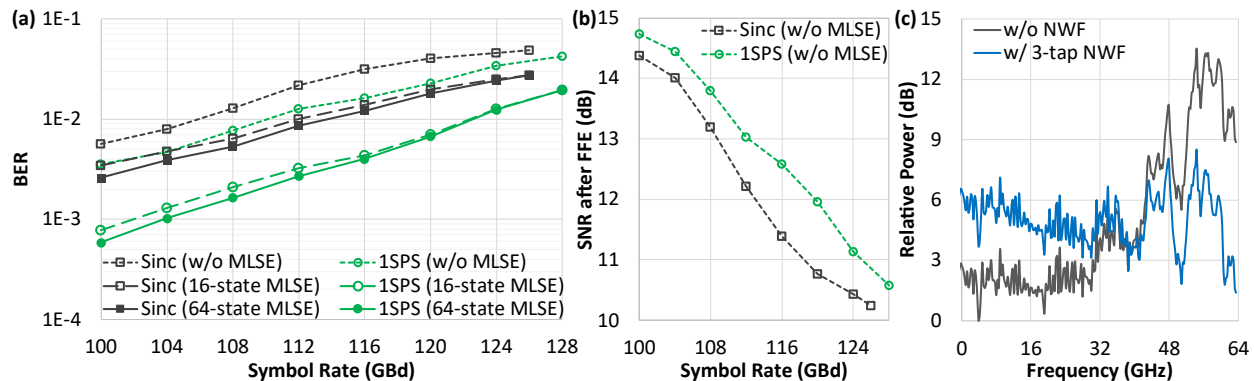
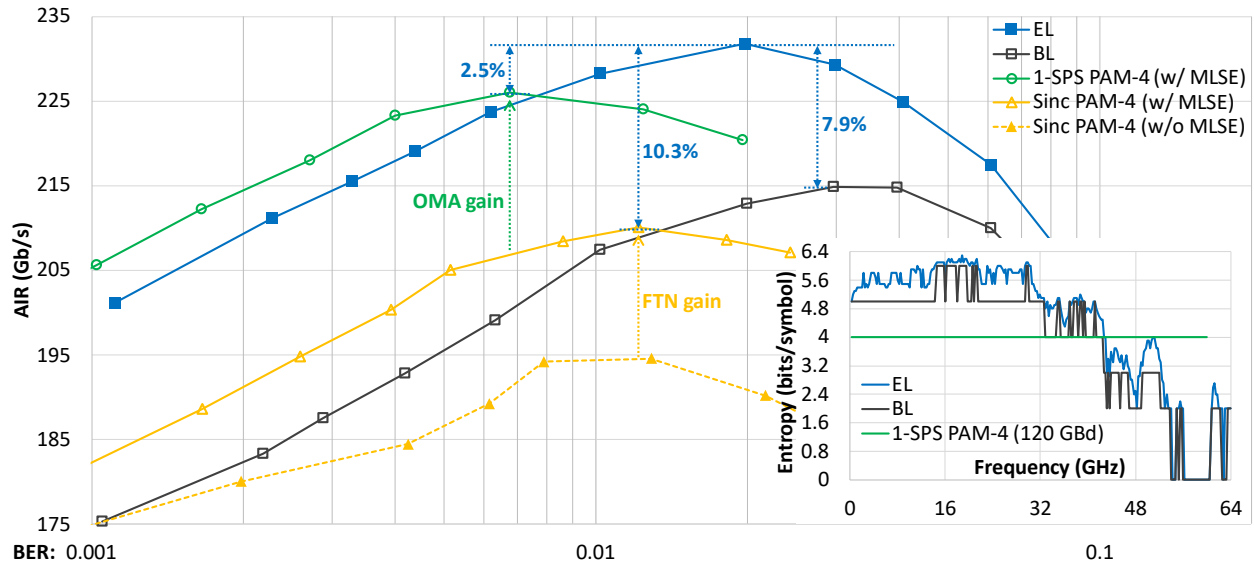


Fig. 2. PAM performance. Comparisons between signals with little (1SPS) or significant (Sinc) peak distortions: (a) BER as a function of symbol rate with or without FTN decoding, (b) SNR after FFE; (c) noise power spectral density with or without NWF for the 1-sps 128-GBd PAM-4 signal.



MLSE) signal with the DMT-BL signal. With the same PAPR between the two, BL improves the maximum AIR by $>10\%$ owing to its capability to accommodate the BWL. In contrast, using FTN decoding to combat the BWL, Sinc PAM-4 achieves a maximum AIR only 2.3% away from that of BL, and even outperforms BL at lower BER region. Further, when the PAM-4 signal is generated at 1 sps without significant peak distortion, the enhanced OMA for PAM-4 greatly improves its AIR, which results in 5.2% advantage of maximum AIR over BL.

We then compare PAM signals with the DMT-EL signal. EL can achieve the PCS gain over BL even in the PPC system, because the significant PAPR enhancement of IDFT almost converts the PPC to the average power constraint [11]. This results in 7.9% AIR gain over BL in the capacity-approaching region with a BER of around 0.02, and even $>10\%$ gain when the BER is less than 0.01. Such gain is also evidenced in the inset of Fig. 3, where EL loads higher entropies than BL at all subcarriers with the same BER target of 0.02. In Fig. 3, EL also shows higher maximum AIR than the 1-sps PAM-4 signal. The reason is twofold. First, under the PPC, applying common Maxwell-Boltzmann distributed PCS to PAM induces larger signal power penalty than the PCS gain, leading to a net penalty especially for the case with little peak distortion [11] like the 1-sps PAM. This prevents PAM to exploit the PCS gain. Second, the higher frequency resolution of BWL tolerance helps EL better accommodate the colored response than PAM and extends the usable spectrum from 60 to 64 GHz, as indicated in the inset of Fig. 3. The two (1-sps and Sinc) PAM curves in Fig. 3 represent two boundary cases with little and significant peak distortion (*i.e.*, OMA penalty). For real-world electronic transmitters with moderate distortion, the AIR curve may move up/down between these two bounds.

4. Conclusions

In a BWL IM-DD system, EL can achieve higher AIR than FTN-PAM owing to its better adaptation to the colored response and the PCS gain. If the BWL mainly comes from the optical modulator rather than the electronic transmitter, the EL advantage over PAM may be marginal, in which case PAM is more appealing due to its simplicity. In contrast, if the electronic transmitter has strong BWL that induces significant peak distortion (power penalty) to PAM signals, the EL gain may be increased to more than 10%, making DMT a promising option with higher AIR and rate flexibility.

5. References

- [1] S. Randel *et al.*, "Advanced modulation schemes for short-range optical communications," J. Sel. Top. in Quantum Electron. 16, 1280 (2010).
- [2] Y. Kai *et al.*, "Experimental comparison of pulse amplitude modulation (PAM) and discrete multi-tone (DMT) ..." ECOC'2013, Th.1.F.3.
- [3] K. Zhong *et al.*, "Experimental study of PAM-4, CAP-16, and DMT for 100 Gb/s short reach optical ..." Opt. Express 23, 1176 (2015).
- [4] J. Shi *et al.*, "Transmission performance comparison for 100-Gb/s PAM-4, CAP-16, and DFT-S OFDM ..." J. Lightw. Tech. 35, 5127 (2017).
- [5] N. Eiselt *et al.*, "Performance comparison of 112-Gb/s DMT, Nyquist PAM4, and partial-response PAM4 for future 5G Ethernet-based fronthaul architecture," J. Lightw. Tech. 36, 1807 (2018).
- [6] X. Pang *et al.*, "200 Gbps/lane IM/DD technologies for short reach optical interconnects," J. Lightw. Tech. 38, 492 (2020).
- [7] J. Wei *et al.*, "Experimental demonstration of advanced modulation formats for data center networks ..." Opt. Express 28, 35240 (2020).
- [8] Q. Hu *et al.*, "IM/DD beyond bandwidth limitation for data center optical interconnects," J. Lightw. Tech. 37, 4940 (2019).
- [9] D. Che *et al.*, "Higher-order modulation vs faster-than-Nyquist PAM-4 for datacenter IM-DD optics: an AIR comparison under practical bandwidth limits," J. Lightw. Tech. 40, 3347 (2022).
- [10] D. Che *et al.*, "Squeezing out the last few bits from band-limited channels with entropy loading," Opt. Express 27, 9321 (2019).
- [11] D. Che *et al.*, "Does probabilistic constellation shaping benefit IM-DD systems without optical amplifiers?" J. Lightw. Tech. 39, 4997 (2021).
- [12] G. Böcherer, "Achievable rates for probabilistic shaping," arXiv:1707.01134.